Journal of Materials Chemistry B

Accepted Manuscript

ROYAL SOCIETY OF CHEMISTRY

www.rsc.org/materialsB

Journal Name Journal of Materials Chemistry B Dynamic Article Links ►

Cite this: DOI: 10.1039/c0xx00000x

www.rsc.org/xxxxxx

ARTICLE TYPE

Infection-resistant Styrenic Thermoplastic Elastomers that can Switch from Bactericidal Capability to Anti-adhesion

Shuaishuai Yuan[a,c], Yonggang Li[b], Shifang Luan[a,*], Hengchong Shi[a], Shunjie Yan[a,c], Jinghua Yin[a,*]

Received (in XXX, XXX) Xth XXXXXXXXX 20XX, Accepted Xth XXXXXXXXX 20XX

DOI: 10.1039/b000000x

Styrenic thermoplastic elastomers (STPE), particularly for poly(styrene-b-isobutylene-b-styrene) (SIBS), have aroused great interest for the indwelling and implant applications. However, the biomaterial-associated infection is a great challenge for these hydrophobic elastomers. Here, benzyl chloride (BnCl) groups are initially introduced onto SIBS backbone via Friedel-Crafts chemistry, followed by reacting with methyl 3-(dimethylamino) propionate (MAP) to obtain cationic carboxybetaine ester-modified elastomer. The as-prepared elastomer is able to kill bacteria efficiently, while upon the hydrolysis of carboxybetaine esters into zwitterionic groups, the resultant surface has antifouling performances against protein, platelets, erythrocytes, and bacteria. This STPE that switches from bactericidal efficacy during storage to antifouling property in service has great potential in biomedical applications, and is generally applicable to the other styrene-based polymers.

1. Introduction

Styrenic thermoplastic elastomers (STPE) that possess unique physical and biological performances have aroused great interest in biomedical field.[1-3] Of these elastomers, poly(styrene-b-isobutylene-b-styrene) (SIBS) has been widely used in various biomedical applications, such as stent drug controlled release coating, heart valve, urinary tract, and glaucoma shunt, because of its balanced elasticity, thermal stability, processibility, and biocompatibility.[4-7] However, bacteria tend to attach on the hydrophobic surfaces of the STPE-based devices, and finally form biofilms which results in the increased resistance to antimicrobials and host immune system.[8] Therefore, the infection-resistant performances of STPE should be improved for addressing this problem.[9-11]

Many modification approaches have been developed to confer infection-resistant properties to a commercial biomedical polymer, commonly based on bactericidal or bacteria-repelling mechanisms.[12] Various bactericides including but not limited to antibiotics,[13] halamine,[14] cationic polymers,[15-18] silver,[19-20] have been used to actively kill or reduce growth of bacteria. However, drug resistance or poor hemocompatibility is of great concern.[21] Creating antifouling surfaces that passively inhibit the initial bacterial adhesion through the hydration of hydrophilic moieties, e.g., poly(ethylene glycol) (PEG),[22-23] poly(carboxybetaine methacrylate),[24-28] poly(sulfobetaine methacrylate),[29-31] neutral polysaccharides,[32] and poly(N-vinylpyrrolidone),[33] is developed for preventing the device-related infections. To our knowledge, the zwitterionic materials can dramatically reduce nonspecific protein adsorption, cell adhesion, and inhibit the attachment of microbes, because of the excellent hydrophilicity and oxidative stability.[34] It has been demonstrated that pCBMA has undetectable protein adsorption even from undiluted blood plasma and serum, for the strong hydration capacity.[35] Although antifouling surfaces can prevent initial attachment of bacteria, they are powerless against bacteria once microbes adhere onto the surface.[12] Recently, the combination strategy of active bactericidal efficacy and passive antifouling capability into a surface has been proposed.[36-38] Jiang et al. designed a cationic poly(N,N-dimethyl-N-(ethoxycarbonylmethyl)-N-[2'-(methacryloyloxy)ethyl]-ammoniumbromide) (pCBMA-1 C2)-functionalized surface that can kill the adherent bacterial cells at initial stage, and the resultant zwitterionic surface can inhibit surface fouling performance, providing long-term in vivo biocompatibility after the ester end groups is hydrolyzed into anionic carboxylates.[24]

Halomethylation of polystyrene is a facile functionalization strategy that has been applicable for a variety of polystyrenes-based polymers.[39-40] This chemical modification route is particularly attractive, because the aromatic ring pendants can be readily and efficiently modified through electrophilic substitution under mild conditions. In this study, the styrene block in SIBS backbone is first chloromethylated via Friedel-Crafts chemistry, therefore allowing the subsequent immobilization of methyl 3-(dimethylamino) propionate (MAP) to obtain cationic carboxybetaine ester-modified elastomers. The biological performances of the samples were evaluated, including protein adsorption, platelet adhesion, erythrocytes attachment, and antibacterial property.

2. Experimental section

2.1 Materials and reagents

SIBS with 30 wt % PS hard blocks were kindly provided by Kaneka Americas. 1,3,5-Trioxane, tin (IV) chloride, N-cyclohexyl-3-aminopropanesulfonic acid (> 98%, CAPS), trimethylchlorosilane (TMCS), and methyl 3-(dimethylamino) propionate (99 %, MAP) were purchased from Sigma-Aldrich. Fluorescein isothiocyanate (FITC)-labeled bovine serum fibrinogen (BFg), methyl thiazolyl tetrazolium (MTT) and phosphate buffered solution (PBS, 0.1 mol/L, pH = 7.4) were provided by Dingguo Biotechnology (China). Staphylococcus aureus (S. aureus; ATCC 6538), and tryptic soy broth (TSB) were obtained from Dingguo Biotechnology Co., Ltd. The LIVE/DEAD Backlight Bacterial Viability Kit L7012 was purchased from Molecular Probe Inc., Eugene, OR. Dulbecco's modified Eagle's medium (DMEM) and 0.25 wt % trypsin were purchased from Beijing Solarbio Science & Technology. Sterile filtered fetal bovine serum (FBS) was supplied by Beijing Yuanhengjinma Biotechnology. Other reagents were AR grade and all the materials were used as received directly without further purification.

2.2 Chloromethylation of SIBS

Typically, 5.0 g of SIBS and 5.4 g of trioxane (60 mmol) were dissolved in 250 mL of chloroform in a flask to yield a clear solution, and 22.8 mL of TMCS (180 mmol) and 3 mL of tin(IV) chloride (25.8 mmol) were added to the mixture with stirring at 0 °C for 30 min, and kept at room temperature for 6 h. Subsequently, 100 mL of methanol/water solution (50 % v/v) was added to stop the reaction. To obtain chloromethylated-SIBS (SIBS-Cl), the reaction mixture was precipitated in methanol, and purified by several iterations of dissolving/precipitation in chloroform/methanol, and dried overnight in a vacuum oven at room temperature.

2.3 Quaternization

The SIBS-Cl was dissolved in toluene to prepare a 10 wt% solution. The resulting homogeneous solution was poured onto glass plates, and dried at room temperature. The obtained samples were peeled off and placed in a vacuum oven to completely evaporate the residual solvent. The dried samples were immersed into MAP solution for 48 h to introduce quaternary ammonium groups. After rinsing carefully with deionized water, the quaternized-SIBS (Q-SIBS) were dried overnight in a vacuum oven at room temperature.

2.4 Zwitteration

Q-SIBS samples were immersed into N-cyclohexyl-3-amino-propanesulfonic acid (CAPS) buffer (10 mM, pH = 10.0) at 37 °C. CAPS is a non-toxic chemical used as buffering agent in biochemistry. After 3 h hydrolysis, the samples (namely Z-SIBS) were washed by deionized water and dried by vacuum. The as-prepared Z-SIBS samples were directly used in the following experiments without being additional treated with bacteria or other biomolecules.

2.5 Characterization

The ^{1}H-NMR spectra were collected on a Bruker AV 400 M NMR spectrometer with deuterated chloroform as the solvent and tetramethylsilane as the internal standard at room temperature. The molecular weight of the modified copolymer was determined by using a gel permeation chromatography (GPC, Waters 410) with tetrahydrofuran as elution solvent.

ATR-FTIR spectra of the SIBS samples were obtained from a Fourier transform infrared spectrometer (FTIR, BRUKER Vertex 70) with a resolution of 4 cm^{-1} in absorbance mode.

The chemical composition of the samples were characterized by X-ray photoelectron spectroscopy (XPS, VG Scientific ESCA MK II Thermo Avantage V 3.20 analyzer) with Al/K (hν = 1486.6 eV) anode mono-X-ray source. All the samples were completely vacuum-dried prior to use. The releasing angle of the photoelectron for each atom was fixed at 90°. Surface spectra were collected over a range of 0-1200 eV, and high-resolution spectra of C_{1s}, N_{1s}, O_{1s}, and Cl_{1s} regions were collected. The atomic concentrations of the elements were calculated by the corresponding peak areas.

The static water contact angles (WCA) on the samples were carried out at room temperature using a contact angle goniometer (DSA KRUSS GMBH, Hamburg 100) through injecting 2 μL of distilled water on the surfaces. The value of water contact angle was recorded. Five measurements were conducted on each sample to obtain the average value of contact angles.

2.6 Protein adsorption

FITC-labeled BFg was directly used to visually illustrate protein adsorption on the samples. The samples were dipped into the PBS solution containing FITC-labeled BFg (0.1 mg/mL) at 37 °C for 1 h. After rinsing with PBS, drying with a nitrogen flow, the samples were finally observed under confocal laser scanning microscopy (CLSM; LSM 700, Carl Zeiss).

2.7 Blood cell adhesion

Fresh blood collected from a healthy rabbit was mixed immediately with a 3.8 wt % solution of sodium citrate at a dilution ration of 9:1 (The experiments were carried out in accordance with the guidelines issued by the Ethical Committee of the Chinese Academy of Sciences). The blood was centrifuged at 1000 rpm for 15 min to obtain the platelet-rich plasma (PRP) (up) and erythrocytes (bottom). The erythrocytes were suspended by 0.9 wt% normal saline at a dilution ratio of 1:5.

The SIBS samples (1.5 × 1.5 cm^2) were placed into a 6-well polystyrene plate, sterilized by ethanol for 2 h, dried under vacuum at room temperature for 12 h, and then equilibrated by PBS at 37 °C for 2 h. Twenty microliters of fresh PRP or suspended erythrocytes were dropped onto the center of each sample, followed by incubation for 30 min at 37 °C. After being rinsed with PBS moderately, the adherent cells on the samples were fixed by 2.5 wt % glutaraldehyde at 4 °C for 10 h. Finally, the samples were washed with PBS several times and dehydrated with a series of ethanol/water mixtures (10, 30, 50, 70, 90, and 100 vol % ethanol) for 30 min in each step. The samples were observed with a field emitted scanning electron microscopy (FESEM, XL 30 ESEM FEG, FEI Company).

2.8 Antibacterial performance assay

S. aureus were inoculated onto separated agar plates, and incubated overnight at 37 °C. A single colony of S. aureus from

the agar plate was used to inoculate 10 mL of TSB, and cultured for 24 h at 37 °C. These cultures were in turn used to inoculate a 200 mL main culture in TSB, which was grown for 24 h prior to harvesting. The bacteria containing growth broth were then centrifuged at 2700 rpm for 10 min to remove the supernatant.

Bacterial concentration was calculated by testing the absorbance of the cell dispersions at 540 nm relative to a standard calibration curve.[41] An optical density of 1.0 at 540 nm is equivalent to ~10^9 cells/mL. After removing the supernatant, the bacterial cells were diluted with PBS to 10^9 cells/mL. For initial adhesion, the samples were placed in 24-well plates and covered with bacterial suspension (2 mL) at 37 °C. Bacterial suspensions were removed after 60 min, and the samples were gently washed with PBS. For assessing the viability of the adherent bacteria on the SIBS samples, the samples were stained by a combination dye (LIVE/DEAD Bac Light Bacterial Viability Kit) and observed under confocal laser scanning microscopy (CLSM; LSM 700, Carl Zeiss). The LIVE/DEAD BacLight Bacterial Viability assay utilize mixtures of SYTO 9 green fluorescent nucleic acid dye stain and red fluorescent nucleic acid dye propidium iodide (PI). As for this assay, viable (appearing green) and dead (appearing red) bacterial cells can be distinguished with CLSM. The percentage of the occupied area of adhered bacteria from the fluorescent images were counted using Image J software.

2.9 Cytotoxicity assay

The standard methyl thiazolyl tetrazolium (MTT) assay was used to investigate the cytotoxicity of the samples. DMEM supplemented with 10 vol % fetal bovine serum, 4.5 g/L Glucose, 100 units/mL penicillin was used to culture Murine fibroblasts cell line L929. 1 mL of medium containing the DMEM L929 fibroblasts at a density of 10^5 cells/mL were placed in each well of a 24-well plate. The plate was then incubated in a humidified 5 vol % CO_2/95 vol % air incubator at 37 °C for 24 h. The samples (1 cm × 1 cm) were gently placed on top of the cell layer in the well after replacing the medium with a fresh one. The control experiment was carried out using the growth culture medium without the samples. After incubation for another 24 h at 37 °C, the culture medium and samples in each well was removed. Culture medium (900 μL) and MTT solution (5 mg/mL in PBS, 100 μL) were then added to each well. After 4 h of incubation, the MTT solution and medium was removed and dimethyl sulfoxide (DMSO, 1 mL) was added to dissolve the formazan crystals. The optical absorbance at 490 nm was measured through microplate reader. The results were expressed as percentages relative to the optical absorbance obtained in the control experiment.

2.9. Statistical analysis

All data are presented as mean ± standard deviation (SD). The statistical significance was assessed by analysis of variance (ANOVA), * ($p < 0.05$), ** ($p < 0.01$), *** ($p < 0.001$). Each result is an average of at least three parallel experiments.

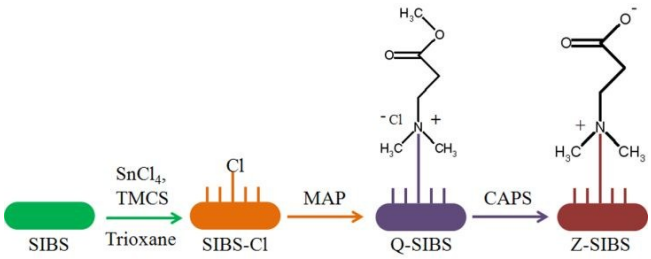

Scheme 1. Preparation of bactericidal and antifouling switchable SIBS samples.

3. Results and discussion

As illustrated in Scheme 1, the SIBS samples that switch from bactericidal capability to anti-adhesion were facilely prepared through chloromethylation and quanternization methods. The surface with homogeneous chlorine could be maintained even though the chloromethylated-SIBS was subjected to additional processing which totally changes the initial shape and morphology, thus it's suitable for practical application. The Q-SIBS could be obtained by simple immersion of the SIBS-Cl in a dilute aqueous solution of MAP at room temperature. This strategy provides a simple, scalable, and efficient method to prepare the infection-resistant STPE that switches from bactericidal capability to anti-adhesion.

3.1 Surface characterization

The SIBS-Cl was prepared by Friedel-Craft reaction with stannic chloride as a catalyst in chloroform solution in presence of trioxane and chlorotrimethylsilane. The ^{1}H NMR spectrum of chloromethyleted SIBS showed the appearance of a new signal at 4.5 ppm corresponding to the $-CH_2Cl$ proton, confirming the chloromethlylation of SIBS at the benzene ring (Fig. 1(a)).[39] The molecular weight of the copolymer changed after the chloromethylation, suggesting the occurrence of cross-linking reactions (Fig. 1(b)). The ATR-FTIR peak around 1265 cm^{-1} attributing to C−Cl pendants on the SIBS−Cl backbones also confirmed the chloromethylation of SIBS (Fig. 2(b)). After the covalent immobilization of MAP, a new peak at about 1726 cm^{-1} (C=O) was obviously observed (Fig. 2(c)). The peak shift from about 1726 cm^{-1} to about 1632 cm^{-1} (COO^-) was found, after the hydrolysis of carboxybetaine esters (Fig. 2(d)).[26]

XPS is a highly surface-specific analytical technique, with typical sampling depths for organic substrates of around 5-10 nm. It can precisely reveal the elemental composition of the substrates surface. Herein, the surface composition of samples was examined by XPS. As shown in Fig. 3, a strong C_{1s} peak at ~284.6 eV and a moderate O_{1s} peak at ~532.3 eV (oxygen contamination) appeared on the SIBS sample, the additional Cl_{2p} peak at ~200 eV was detected on the SIBS-Cl samples. As for the Q-SIBS sample, the appearance of a new N_{1s} peak at ~400 eV was a concrete indication of the quaternization reaction, and the atom composition of Cl_{2p} (2.70 %) was close to that of N_{1s} (2.86 %) (Table 1).

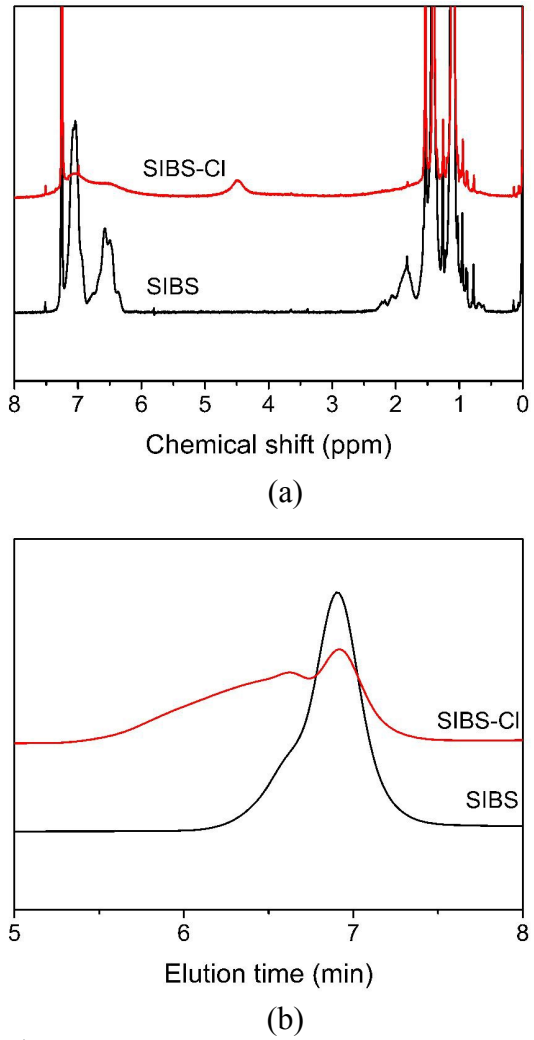

Fig. 1. ^{1}H-NMR spectra (a) and GPC elution curves (b) of SIBS, and SIBS-Cl.

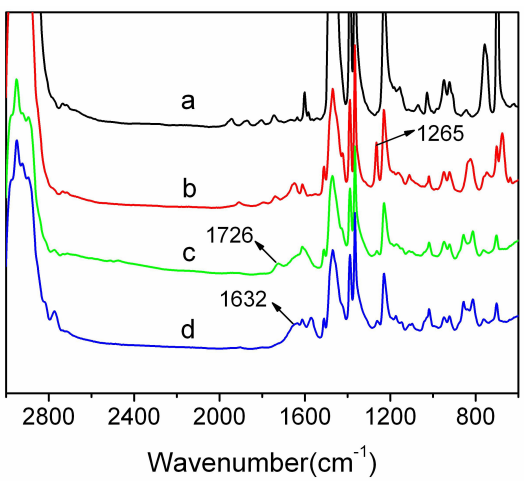

Fig. 2. ATR-FTIR spectra of (a) virgin SIBS, (b) SIBS-Cl, (c) Q-SIBS, and (d) Z-SIBS.

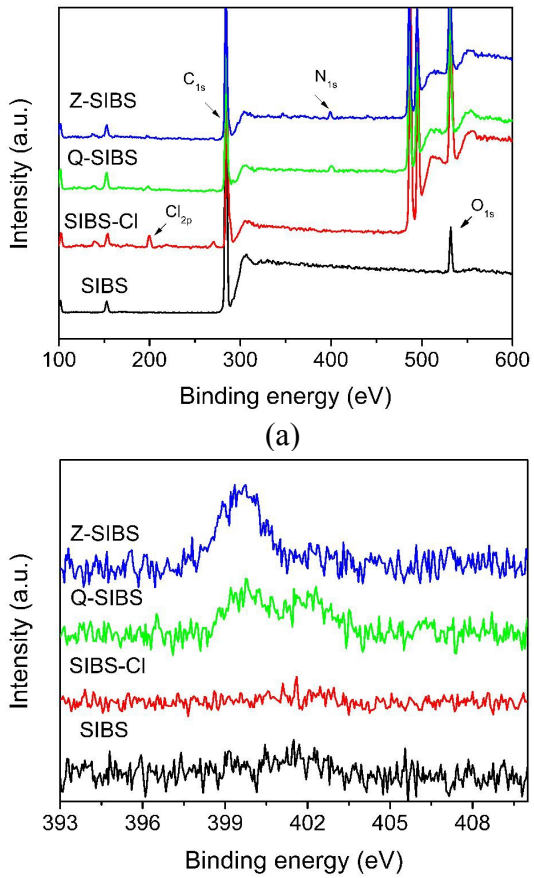

Fig.3. XPS curves (a) and high-resolution N_{1s} spectra (b) of the samples.

Table 1 Analysis of XPS for the samples.

Sample	Composition (atom %)			
	C	O	Cl	N
SIBS	85.92	14.08	-	-
SIBS-Cl	73.70	23.28	3.02	-
Q-SIBS	72.12	22.32	2.70	2.86
Z-SIBS	77.99	18.60	0.42	2.99

3.2 In vitro response of protein, platelet, and erythrocyte

Biological interactions between a host tissue and a biomedical polymer mainly occur at the interface. Upon contacting with bloodstream, a cascade of events including protein adsorption, platelet and erythrocyte adhesion, are initiated, therefore resulting in thrombus.[42] In addition, protein adsorption and the subsequent formation of a layer of protein on the surfaces of biological implants provide a conditioning layer for bacterial attachment and subsequent biofilm formation.

Herein, CLSM was used to visualize the FITC-labeled BFg protein adsorption (Fig. 5). Fibrinogen (BFg) is one of the most abundant serum proteins, and the adsorbed BFg can convert into fibrin during blood clot formation.[9] BFg is negatively charged in PBS solution because its isoelectric point is ~5.6, while the Q-SIBS surface is positively charged. Thus, although the Q-SIBS sample (a WCA of 75° in Fig. 4) was much more hydrophilic than the virgin SIBS sample (a WCA of 106° in Fig. 4), it showed a larger amount of FITC-labeled BFg protein adsorption than that on the virgin SIBS sample, mainly attributing to the electrostatic attraction. In contrast, protein adsorption on the hydrophilic Z-

SIBS sample (a WCA of 40° in Fig. 4) was significantly resisted, owing to its capacity to form a hydration layer capable of disrupting hydrophobic interactions between proteins and the surface.

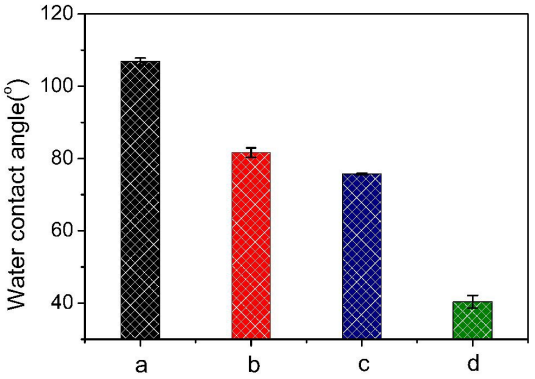

Fig. 4. Water contact angles of (a) virgin SIBS, (b) SIBS-Cl, (c) Q-SIBS, and (d) Z-SIBS.

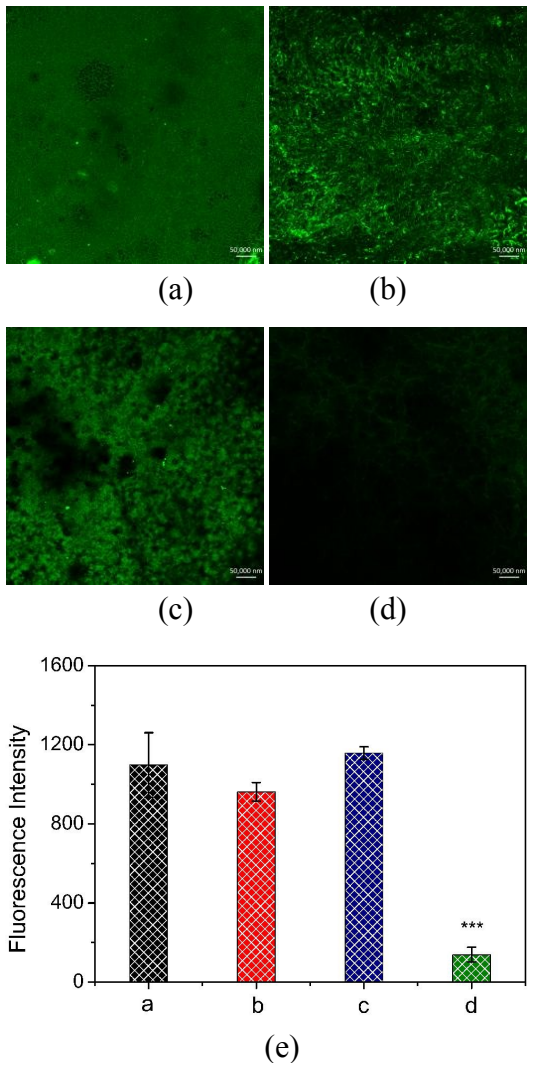

Fig. 5. Representative CLSM images of FITC-labeled BFg adsorption on the samples. (a) virgin SIBS, (b) SIBS-Cl, (c) Q-SIBS, (d) Z-SIBS. The fluorescent intensity of the samples after incubation in FITC-labeled BFg for 1 h (e). Significant difference, Z-SIBS compared with the other samples, *** ($P < 0.001$). (The error bars: standard deviations, n = 3)

It is well known that blood coagulation starts on biomaterial surfaces where platelets aggregate.[43] Here, the adherent blood cells were observed by SEM. As shown in Fig. 6, a large number of activated platelets (the formation of pseudopodia) were adhered on the virgin SIBS, SIBS-Cl and Q-SIBS samples. In contrast, the hydrophilic carboxybetaine quickly formed hydration layer, and therefore, just a few platelets were observed on the Z-SIBS sample.

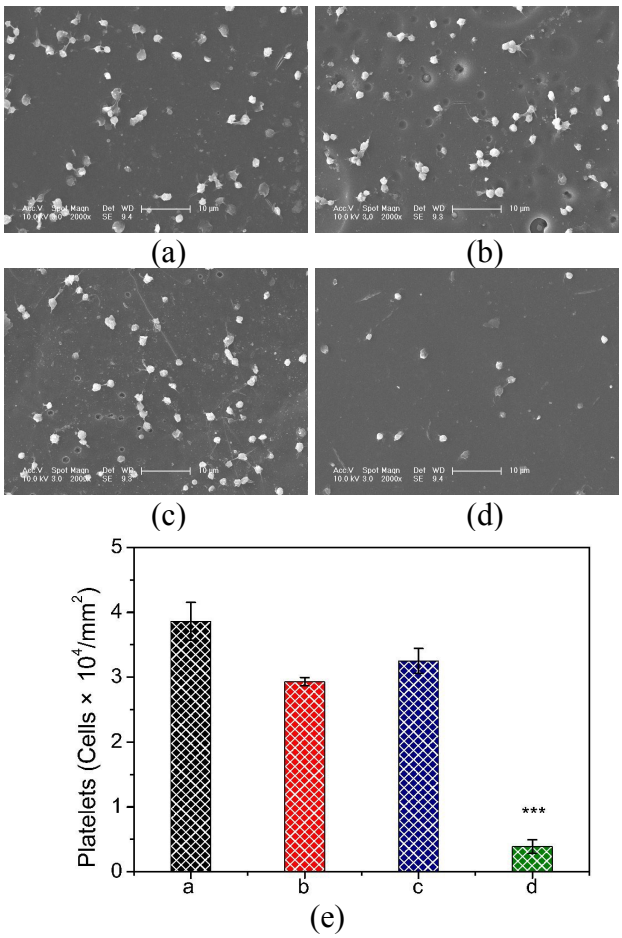

Fig. 6. Representative SEM images of platelets adhesion on (a) virgin SIBS, (b) SIBS-Cl, (c) Q-SIBS, and (d) Z-SIBS samples. The statistical number of adherent platelets (e). (The error bars: standard deviations, n = 3). Significant difference, Z-SIBS compared with the other samples, *** ($P < 0.001$). (The error bars: standard deviations, n = 3)

The erythrocytes are the most abundant cells in the blood. They look like a biconcave disc with central depression on both sides. Because of the deformability, they collide during flow with platelet, and protein, driving them toward the surfaces. The hemolysis of erythrocytes may be aggravated when they come in contact with a foreign implant.[44] The broken erythrocytes can intensify platelets assembly, therefore accelerating the formation of thrombus. As shown in Fig. 7, in comparison to the virgin SIBS, the number of erythrocytes on the SIBS-Cl surfaces was decreased to ~1.3 × 10^4/mm^2. Due to the positive charge property, the number of erythrocytes on the Q-SIBS sample (~2 × 10^4/mm^2) was larger than that of the SIBS-Cl samples.[45] As

expected, the zwitterionic surfaces (Z-SIBS) presented good antifouling property against the erythrocytes (Fig. 5(d, and e)).

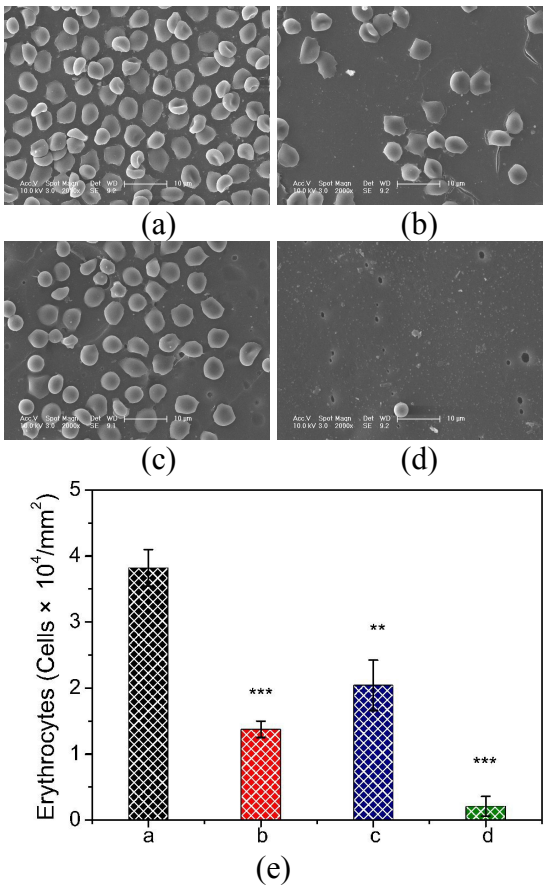

Fig. 7. Representative SEM images of erythrocyte adhesion on (a) virgin SIBS, (b) SIBS-Cl, (c) Q-SIBS, and (d) Z-SIBS samples. The statistical number of adherent erythrocytes (e) (The error bars: standard deviations, n = 3). Significant difference, the samples compared with the virgin SIBS, ** ($p < 0.01$),*** ($P < 0.001$). (The error bars: standard deviations, n = 3)

3.3 Antibacterial Performance

Attachment of bacteria to a surface is the initial procedure in the pathogenesis of foreign-body-related infections. Following the irreversible attachment on a surface, bacteria reproduce, aggregate and grow into microcolonies, and finally differentiate into mature biofilms. Thus, suppressing the initial adhesion of bacteria is critical to avoid the bacterial-related infection. S. aureus is a Gram-positive bacterium, and it has long been recognized as a kind of important microbes that cause disease in humans.[46] Herein, S. aureus adhesion on the samples was conducted in PBS buffer for 60 mim, since bacterial behaviors were simplified in PBS circumstance, and the irreversible bacterial attachment occurred during this period. The adherent bacteria were assessed by CLSM images (Fig. 8). In the assay, bacteria that stain green are live cells, while bacteria that stain red are dead cells. As shown in Fig. 8, the hydrophobic SIBS surface was highly susceptible to S. aureus. A large amount of bacterial cells adhered readily on the virgin SIBS surface (percentages of S. aureus adhesion area: ~55.1%), and most of the bacteria were live (percentages of live S. aureus adhesion area: ~53.0%). Although the Q-SIBS sample had a large percentage of S. aureus adhesion area (~35.5%), most of the bacteria were dead (percentages of live S. aureus adhesion area: ~6.1%). The anibacterial mechanism of quaternary-ammonium-compounds (QACs) in solution is based on the membrane interdigitation over the entire surface of a bacterium. However, immobilized QAC-molecules locally enhance the adhesion forces between a bacterium and a surface to a lethally strong attraction, causing reduced growth, stress-induced deactivation and localized removal of membrane lipids, eventually leading to cell death[15, 38, 47] The immobilized QACs molecules disrupt the bacteria membranes without developing antimicrobial resistance. The zwitterionic Z-SIBS surfaces had the highest resistance to bacteria adhesion (Percentage of S. aureus adhesion area: ~5.2%).

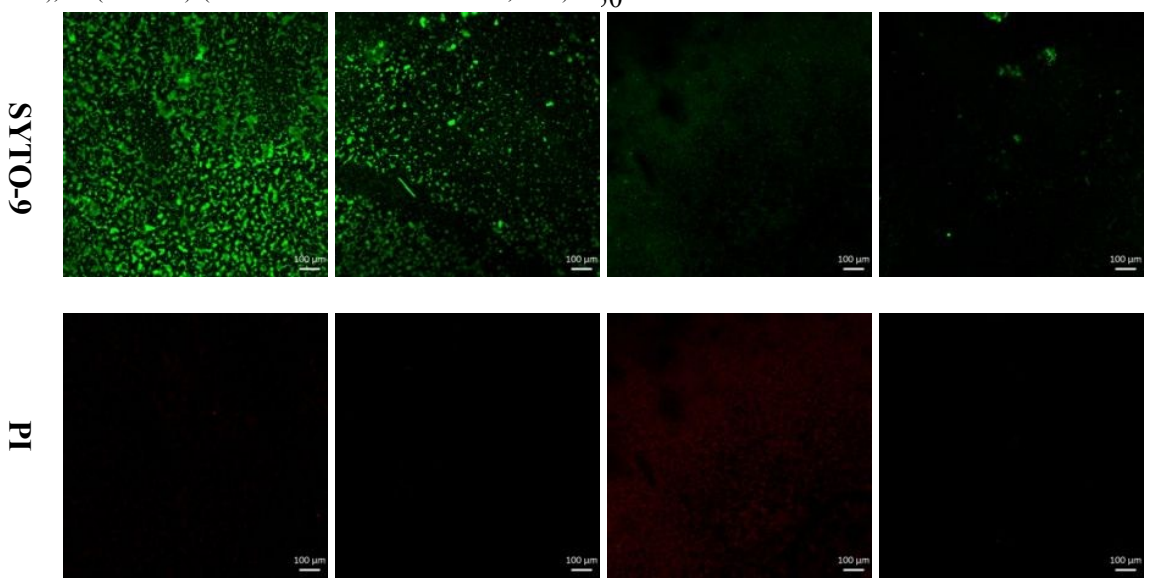

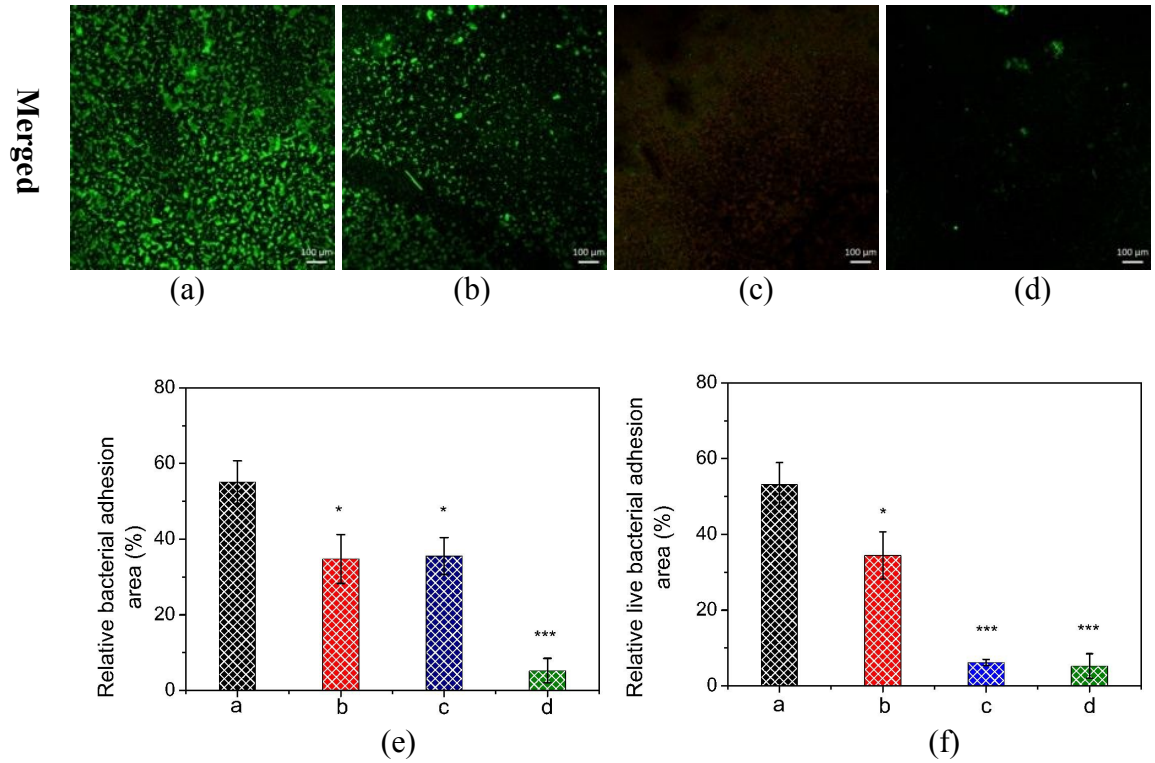

Fig. 8. Representative CLSM images of S. aureus adhesion on (a) virgin SIBS, (b) SIBS-Cl, (c) Q-SIBS, and (d) Z-SIBS samples. Percentages of S. aureus adhesion area (e) and percentages of live S. aureus adhesion area (f). Scale bar is 100 μm. The samples were exposed to a PBS suspension of bacteria (10^9 cells mL^{-1}) for 60 min.. Significant difference, the samples compared with the virgin SIBS, * ($p < 0.05$), *** ($P < 0.001$). (The error bars: standard deviations, n = 3)

3.4. Cytotoxicity assays

The cytotoxicity of samples was evaluated by an MTT assay,[11] since a series of chemicals are used during the preparation procedure. The samples were placed directly on L929 cells and cultured in vitro for 24 h, with tissue culture polystyrene dish as control. As shown in Fig. 9, SIBS and Z-SIBS samples had a high viability(~98 % and ~95 %), confirming the minimal cytotoxicity. In contrast, the positively charged Q-SIBS induced cell death, presenting the lowest cell viability (~88 %). However, unlike bacteria membranes, the outer leaflet of the L929 cell membrane lacks anionic lipids that have much less Coulombic attractive force to disrupt mammalian cells when they are in contact with Q-SIBS sample. These results also confirmed that the reduction of cell adhesion on the Z-SIBS surfaces is attributed to the anti-adhesive property, rather than their cytotoxicity.

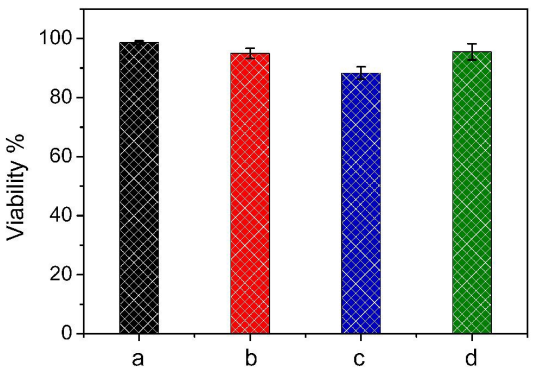

Fig. 9. Cytotoxicity of (a) virgin SIBS, (b) SIBS-Cl, (c) Q-SIBS, (d) Z-SIBS samples to L929 cells by MTT assay. (The error bars: standard deviations, n = 3)

Conclusions

In this work, we proposed a facile strategy to prepare cationic carboxybetaine ester-modified SIBS elastomer. Benzyl chloride (BnCl) groups were initially introduced onto SIBS backbones via Friedel-Crafts chemistry, followed by reacting with methyl 3-(dimethylamino) propionate (MAP). The as-prepared elastomer had capability to kill the adherent bacteria, while after the hydrolysis of carboxybetaine esters into zwitterionic groups; the resultant surface had antifouling performances against protein, platelets, erythrocytes, and bacteria. This STPE that switched from bactericidal efficacy during storage to antifouling property before service had great potential in biomedical applications, and was generally applicable to the other styrene-based polymers.

Acknowledgments

The authors acknowledge the financial support of the National Natural Science Foundation of China (Projects numbers: 51473167, and 51273200), Chinese Academy of Sciences-Wego Group High-tech Research & Development Program (ZKYWG2013-01), and Scientific Development Program of Jilin Province (20130102064JC).

Notes and references

[a] *State Key Laboratory of Polymer and Chemistry, Changchun Institute of Applied Chemistry, Chinese Academy of Sciences, Changchun 130022,*

People's Republic of China. Fax: +86 431 85262109; Tel: +86 431 85262109; E-mail: sfluan@ciac.ac.cn; yinjh@ciac.ac.cn
[b] Wego Holding Company Limited, Weihai 264210, PR China
[c] University of Chinese Academy of Sciences, Beijing 100049, PR China
Republic of China

1. S. F. Luan, J. Zhao, H. W. Yang, H. C. Shi, J. Jin, X. M. Li, J. C. Liu, J. W. Wang, J. H. Yin and P. Stagnaro, *Colloids Surf., B*, 2012, 93, 127-134.
2. J. E. Puskas, E. A. Foreman-Orlowski, G. T. Lim, S. E. Porosky, M. M. Evancho-Chapman, S. P. Schmidt, M. El Fray, M. Piatek, P. Prowans and K. Lovejoy, *Biomaterials*, 2010, 31, 2477-2488.
3. H. W. Yang, S. F. Luan, J. Zhao, H. C. Shi, X. M. Li, L. J. Song, J. Jin, Q. Shi, J. H. Yin, D. Shi and P. Stagnaro, *Polymer*, 2012, 53, 1675-1683.
4. J. E. Puskas and Y. H. Chen, *Biomacromolecules*, 2004, 5, 1141-1154.
5. G. T. Lim, J. E. Puskas, D. H. Reneker, A. Jakli and W. E. Horton, *Biomacromolecules*, 2011, 12, 1795-1799.
6. L. Pinchuk, G. J. Wilson, J. J. Barry, R. T. Schoephoerster, J. M. Parel and J. P. Kennedy, *Biomaterials*, 2008, 29, 448-460.
7. M. El Fray, P. Prowans, J. E. Puskas and V. Altstädt, *Biomacromolecules*, 2006, 7, 844-850.
8. A. L. Hook, C. Y. Chang, J. Yang, J. Luckett, A. Cockayne, S. Atkinson, Y. Mei, R. Bayston, D. J. Irvine, R. Langer, D. G. Anderson, P. Williams, M. C. Davies and M. R. Alexander, *Nat. Biotechnol*, 2012, 30, 868-875.
9. S. Yuan, J. Zhao, S. Luan, S. Yan, W. Zheng and J. Yin, *ACS Appl. Mater. Interfaces*, 2014, 6, 18078-18086.
10. S. S. Yuan, Z. H. Li, J. Zhao, S. F. Luan, J. Ma, L. J. Song, H. C. Shi, J. Jin and J. H. Yin, *RSC Adv.*, 2014, 4, 31481-31488.
11. S. Yuan, S. Luan, S. Yan, H. Shi and J. Yin, *ACS Appl. Mater. Interfaces*, 2015, 7, 19466-19473.
12. N. Hadjesfandiari, K. Yu, Y. Mei and J. N. Kizhakkedathu, *J. Mater. Chem. B*, 2014, 2, 4968-4978.
13. N. Aumsuwan, M. S. McConnell and M. W. Urban, *Biomacromolecules*, 2009, 10, 623-629.
14. J. Luo, N. Porteous, J. Lin and Y. Sun, *J. Bioact. Compat. Polym.*, 2015, 30, 157-166.
15. X. Ding, C. Yang, T. P. Lim, L. Y. Hsu, A. C. Engler, J. L. Hedrick and Y. Y. Yang, *Biomaterials*, 2012, 33, 6593-6603.
16. I. Perelshtein, E. Ruderman, N. Perkas, T. Tzanov, J. Beddow, E. Joyce, T. J. Mason, M. Blanes, K. Molla, A. Patlolla, A. I. Frenkel and A. Gedanken, *J. Mater. Chem. B*, 2013, 1, 1968-1976.
17. F. G. Jiang, C. K. Yeh, J. C. Wen and Y. Y. Sun, *Adv. Healthc. Mater.*, 2015, 4.
18. P. Petkova, A. Francesko, M. M. Fernandes, E. Mendoza, I. Perelshtein, A. Gedanken and T. Tzanov, *ACS Appl. Mater. Interfaces*, 2014, 6, 1164-1172.
19. Z. B. Cao, X. B. Sun, J. R. Yao and Y. Y. Sun, *J. Bioact. Compat. Pol.*, 2013, 28, 398-409.
20. A. Zille, M. M. Fernandes, A. Francesko, T. Tzanov, M. Fernandes, F. R. Oliveira, L. Almeida, T. Amorim, N. Carneiro, M. F. Esteves and A. P. Souto, *ACS Appl. Mater. Interfaces*, 2015, 7, 13731-13744.
21. L. Mi and S. Y. Jiang, *Biomaterials*, 2012, 33, 8928-8933.
22. F. J. Xu, L. Y. Liu, W. T. Yang, E. T. Kang and K. G. Neoh, *Biomacromolecules*, 2009, 10, 1665-1674.
23. H. W. Ma, J. H. Hyun, P. Stiller and A. Chilkoti, *Adv. Mater.*, 2004, 16, 338-+.
24. G. Cheng, H. Xite, Z. Zhang, S. F. Chen and S. Y. Jiang, *Angew. Chem., Int. Ed.*, 2008, 47, 8963-8966.
25. Z. Cao, L. Mi, J. Mendiola, J. R. Ella-Menye, L. Zhang, H. Xue and S. Jiang, *Angew. Chem., Int. Ed.*, 2012, 51, 2602-2605.
26. J. Zhao, L. J. Song, Q. Shi, S. F. Luan and J. H. Yin, *ACS Appl. Mater. Interfaces*, 2013, 5, 5260-5268.
27. W. F. Lin, G. L. Ma, F. Q. Ji, J. Zhang, L. G. Wang, H. T. Sun and S. F. Chen, *J. Mater. Chem. B*, 2015, 3, 440-448.
28. H. Y. Yin, T. Akasaki, T. L. Sun, T. Nakajima, T. Kurokawa, T. Nonoyama, T. Taira, Y. Saruwatari and J. P. Gong, *J. Mater. Chem. B*, 2013, 1, 3685-3693.
29. S. Y. Jiang and Z. Q. Cao, *Adv. Mater.*, 2010, 22, 920-932.
30. C. D. Blanco, A. Ortner, R. Dimitrov, A. Navarro, E. Mendoza and T. Tzanov, *Acs Appl Mater Inter*, 2014, 6, 11385-11393.
31. W. W. Zhao, Q. Ye, H. Y. Hu, X. L. Wang and F. Zhou, *J. Mater. Chem. B*, 2014, 2, 5352-5357.
32. M. Li, K. G. Neoh, E. T. Kang, T. Lau and E. Chiong, *Adv. Funct. Mater.*, 2014, 24, 1631-1643.
33. J. H. Jiang, L. P. Zhu, L. J. Zhu, H. T. Zhang, B. K. Zhu and Y. Y. Xu, *ACS Appl. Mater. Interfaces*, 2013, 5, 12895-12904.
34. A. M. Alswieleh, N. Cheng, I. Canton, B. Ustbas, X. Xue, V. Ladmiral, S. J. Xia, R. E. Ducker, O. El Zubir, M. L. Cartron, C. N. Hunter, G. J. Leggett and S. P. Armes, *J. Am. Chem. Soc.*, 2014, 136, 9404-9413.
35. J. Ladd, Z. Zhang, S. Chen, J. C. Hower and S. Jiang, *Biomacromolecules*, 2008, 9, 1357-1361.
36. Q. Yu, Z. Q. Wu and H. Chen, *Acta Biomater*, 2015, 16, 1-13.
37. L. Mi and S. Y. Jiang, *Angew. Chem., Int. Ed.*, 2014, 53, 1746-1754.
38. S. Q. Liu, C. Yang, Y. Huang, X. Ding, Y. Li, W. M. Fan, J. L. Hedrick and Y. Y. Yang, *Adv. Mater.*, 2012, 24, 6484-6489.
39. S. Itsuno, K. Uchikoshi and K. Ito, *J. Am. Chem. Soc.*, 1990, 112, 8187-8188.
40. T. L. Li, F. L. Ning, J. W. Xie, D. Y. Chen and M. Jiang, *Polym. J.*, 2002, 34, 529-533.
41. W. J. Yang, T. Cai, K. G. Neoh, E. T. Kang, G. H. Dickinson, S. L. M. Teo and D. Rittschof, *Langmuir*, 2011, 27, 7065-7076.
42. G. Gunkel and W. T. S. Huck, *J. Am. Chem. Soc.*, 2013, 135, 7047-7052.
43. H. J. Busscher, H. C. van der Mei, G. Subbiahdoss, P. C. Jutte, J. J. A. M. van den Dungen, S. A. J. Zaat, M. J. Schultz and D. W. Grainger, *Sci. Transl. Med.*, 2012, 4. 153ra132.
44. H. Jiang, X. B. Wang, C. Y. Li, J. S. Li, F. J. Xu, C. Mao, W. T. Yang and J. Shen, *Langmuir*, 2011, 27, 11575-11581.
45. Q. He, K. Gong, Q. Ao, T. Ma, Y. F. Yan, Y. D. Gong and X. F. Zhang, *J. Biomater. Appl.*, 2013, 27, 1032-1045.
46. S. Goswami, D. Thiyagarajan, S. Samanta, G. Das and A. Ramesh, *J. Mater. Chem. B*, 2015, 3, 7068-7078.
47. L. A. T. W. Asri, M. Crismaru, S. Roest, Y. Chen, O. Ivashenko, P. Rudolf, J. C. Tiller, H. C. van der Mei, T. J. A. Loontjens and H. J. Busscher, *Adv. Funct. Mater.*, 2013, 3, 346-355.

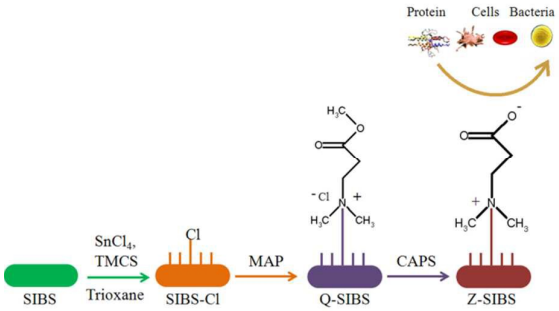

Infection-resistant styrenic thermoplastic elastomers that can switch from bactericidal capability to anti-adhesion are facilely chloromethylated, followed by quaternization with methyl 3-(dimethylamino) propionate.